JOURNAL OF GEOPHYSICAL RESEARCH, VOL. 108, NO. D24, 4799, doi:10.1029/2003JD003824, 2003

Observed and modeled relationships among Arctic climate variables

Yonghua Chen, James R. Miller, and Jennifer A. Francis
Institute of Marine and Coastal Sciences, Rutgers University, New Brunswick, New Jersey, USA

Gary L. Russell and Filipe Aires
NASA/Goddard Institute for Space Studies, New York, New York, USA

Received 2 June 2003; revised 4 September 2003; accepted 11 September 2003; published 31 December 2003.

[1] The complex interactions among climate variables in the Arctic have important implications for potential climate change, both globally and locally. Because the Arctic is a data-sparse region and because global climate models (GCMs) often represent Arctic climate variables poorly, significant uncertainties remain in our understanding of these processes. In addition to the traditional approach of validating individual variables with observed fields, we demonstrate that a comparison of covariances among interrelated parameters from observations and GCM output provides a tool to evaluate the realism of modeled relationships between variables. We analyze and compare a combination of conventional observations, satellite retrievals, and GCM simulations to examine some of these relationships. The three climate variables considered in this study are surface temperature, cloud cover, and downward longwave flux. Results show that the highest correlations between daily changes in pairs of variables for all three data sets occur between surface temperature and downward longwave flux, particularly in winter. There is less variability in GCM output, in part, because there is greater spatial averaging. Although the satellite products can be used to examine some of these relationships, additional work may be needed to ensure consistency between changes in radiative components of the energy budget and other retrieved quantities. The GCM's relationships between variables agree well with in situ observations, which provides some confidence that the GCM's representation of present-day climate is reasonable in high northern latitudes. *INDEX TERMS:* 3349 Meteorology and Atmospheric Dynamics: Polar meteorology; 3359 Meteorology and Atmospheric Dynamics: Radiative processes; 9315 Information Related to Geographic Region: Arctic region; 1694 Global Change: Instruments and techniques; *KEYWORDS:* Arctic, radiation, global climate model, feedback, validation, remote sensing

Citation: Chen, Y., J. R. Miller, J. A. Francis, G. L. Russell, and F. Aires, Observed and modeled relationships among Arctic climate variables, *J. Geophys. Res.*, *108*(D24), 4799, doi:10.1029/2003JD003824, 2003.

1. Introduction

[2] Complex exchanges of energy and water among the ocean, sea ice, and atmosphere cause the Arctic climate system to be particularly sensitive to climate change because clouds, snow, and sea ice introduce a host of feedbacks, some of which have powerful global effects [e.g., *Curry et al.*, 1996]. Some of the changes observed during recent decades in the oceanic and terrestrial northern high latitudes are summarized in *Serreze* [2000]. Among these are significant warming in most Arctic land areas, downward trends in sea ice cover, and negative snow anomalies over both continents.

[3] Modeling studies indicate that the polar regions play a disproportionately important role in governing the global climate system [e.g., *Ingram et al.*, 1989; *Rind et al.*, 1995]. Simulations of present-day climate by the many existing global climate models differ widely from each other, especially in high latitudes. *Gates et al.* [1999] show a comparison of winter sea level pressure and cloud cover in present-day conditions computed by 31 different global climate models (GCMs). The most probable causes for the large disagreements in polar regions are related to unrealistic parameterizations of the myriad of feedbacks. Despite these significant differences among models, GCMs generally agree that the Arctic will experience the strongest warming in response to increasing concentrations of greenhouse gases [e.g., *Holland and Bitz*, 2003]. Increases in temperature are expected to be accompanied by changes in a wide range of environmental parameters, such as sea ice extent and thickness, cloud amount, precipitation, and river runoff, but the magnitudes and even signs of some of these changes are in dispute.

[4] Our understanding of the interactions and feedbacks among the components of the Arctic climate system can be significantly advanced by integrating new observations of Arctic climate variables with global coupled, atmosphere-ocean-ice models. Model-only studies are limited by being insufficiently validated against observations, and observation-only studies are often limited by data scarcity or by

0148-0227/03/2003JD003824

poor spatial and temporal sampling. A recent Intergovernmental Panel on Climate Change (IPCC) comparison of GCMs with and without sea ice dynamics showed no difference in simulation quality, apparently because model differences in surface forcing overwhelmed the results [*Intergovernmental Panel on Climate Change*, 2001]. Recently available Arctic data sets, such as from satellite sounders and imagers (e.g., Polar Pathfinder data sets from TOVS [*Francis and Schweiger*, 2000] and the Advanced Very High Resolution Radiometer (AVHRR) [*Maslanik et al.*, 1997]) field campaigns (e.g., the Surface Heat Budget of the Arctic Ocean (SHEBA) [*Uttal et al.*, 2002]), and Russian drifting ice stations, offer new opportunities to evaluate and improve GCM simulations. Even though their record lengths are limited, these observations viewed separately and in concert can be used to improve the accuracy of numerical models by evaluating the realism of their output and analyzing feedback mechanisms and relationships among climate variables. While observations and GCMs individually offer limited ability to study these relationships, the combination of the two constitutes a valuable tool.

[5] In this paper we compare observations with simulated fields from the GCM of *Russell et al.* [1995]. The model conserves water, includes many important high-latitude feedbacks, and is internally self consistent. The observations are from the SHEBA experiment [*Uttal et al.*, 2002] and satellite retrievals. We compare modeled and observed relationships among several different climate variables to determine whether the GCM realistically represents these interactions and whether the satellite-derived relationships are consistent with the in situ SHEBA observations. A previous study that compared relationships among observed and GCM climate variables in the Arctic was by *McGinnis and Crane* [1994] using a rotated principal component analysis. Their focus was on large-scale spatial relationships, while the focus in the present study is on local, short-term, temporal relationships based on daily changes in each variable. These relationships and sensitivities are the controlling factors for feedbacks. As pointed out in *Aires and Rossow* [2003], if the modeled sensitivities differ from reality, so may the feedbacks that involve those variables. The principal objective of this study is to extend observational and model studies by examining the relationships among climate variables and the processes and feedbacks that are most important in the high-latitude climate system, including an attempt to quantify some of these relationships.

[6] Although there are many climate variables to consider, the focus here will be on surface air and skin temperature, cloud cover, and downward longwave flux (DLF). The analysis of relationships among these variables can be separated into three components. The first is to subset satellite retrievals and GCM output for the SHEBA region and time period. The second is to compare SHEBA measurements directly with satellite retrievals from the Television Infrared Observation Satellite (TIROS) Operational Vertical Sounder (TOVS) and with GCM output. The final component is to compare relationships among climate variables measured by SHEBA to those from TOVS and the GCM. In the following two sections of the paper we describe the global climate model and the observational data sets. Comparisons of parameters from GCM output, TOVS satellite retrievals, and in situ measurements at the SHEBA site are presented in section 4. Our conclusions are given in Section 5, where we provide Table 2 to help summarize and quantify the results.

2. Climate Model Description

[7] We use the global synchronously coupled atmosphere-ocean-ice model developed by *Russell et al.* [1995]. A model description is available at http://aom.giss.nasa.gov/DOC/ATMOCEAN.TXT. The model has 9 vertical layers in the atmosphere and 13 in the ocean. The horizontal resolution for both the atmosphere and ocean is 4° in latitude by 5° in longitude. Heat, water vapor, and salt have finer resolution because these quantities have both mean values and directional gradients inside each grid cell that are used in their advection. Atmospheric condensation and ocean vertical mixing are performed on $2° \times 2.5°$ horizontal resolution. The ocean model includes the k profile parameterization (KPP) vertical mixing scheme of *Large et al.* [1994], does not use flux adjustments, does not use the Boussinesq approximation, has a free surface, and conserves mass and not volume. Freshwater is removed from or added to the upper layer of the ocean by evaporation, precipitation and river discharge. Continental runoff and glacial ice melting eventually find their way back to the oceans via a river network. Sea ice, which may fractionally cover any ocean grid cell, has both thermodynamic and dynamic components [*Miller and Russell*, 1997].

[8] The modeled cloud cover is diagnostically determined from the cloud optical depths that, in turn, depend upon the local temperature and the square root of the condensate leaving each grid cell. Global constants of proportionality (between optical depth and condensate) for each process (moist convection or large-scale condensation) and for each phase (liquid or ice) are chosen to match current radiative observations. If the vertically integrated optical depth is less than 1, no cloud cover is tabulated for that time step. When the vertically integrated optical depth exceeds 1, a cloud is present. The cloud top is assumed to be in the layer at which the optical depth, vertically integrated from the top, first exceeds 1. Both shortwave and longwave radiation are calculated using the correlated k distribution method described in *Hansen et al.* [1983]. In that method, radiative calculations are performed on discontinuous domains that are grouped according to absorption coefficient strength.

[9] The GCM fields used in this study are a 22-year period of a 150-year control simulation for present climate conditions in which atmospheric greenhouse gases are fixed at 1950 levels. Because the model assimilates no data, the years designated as the control simulation (1950–2100) have no relationship to actual years from 1950 to the present, but they are used to measure climate drift for climate change experiments [e.g., *Miller and Russell*, 2000, 2002]. The GCM record used in the relationship study is for the period from 1979 to 1998, which corresponds to the period of record for the TOVS data described in the next section, but not to actual conditions in any particular year.

3. Observational Data Sets

[10] Two different data sets are used in the analysis and described briefly in this section. The TOVS instrument has

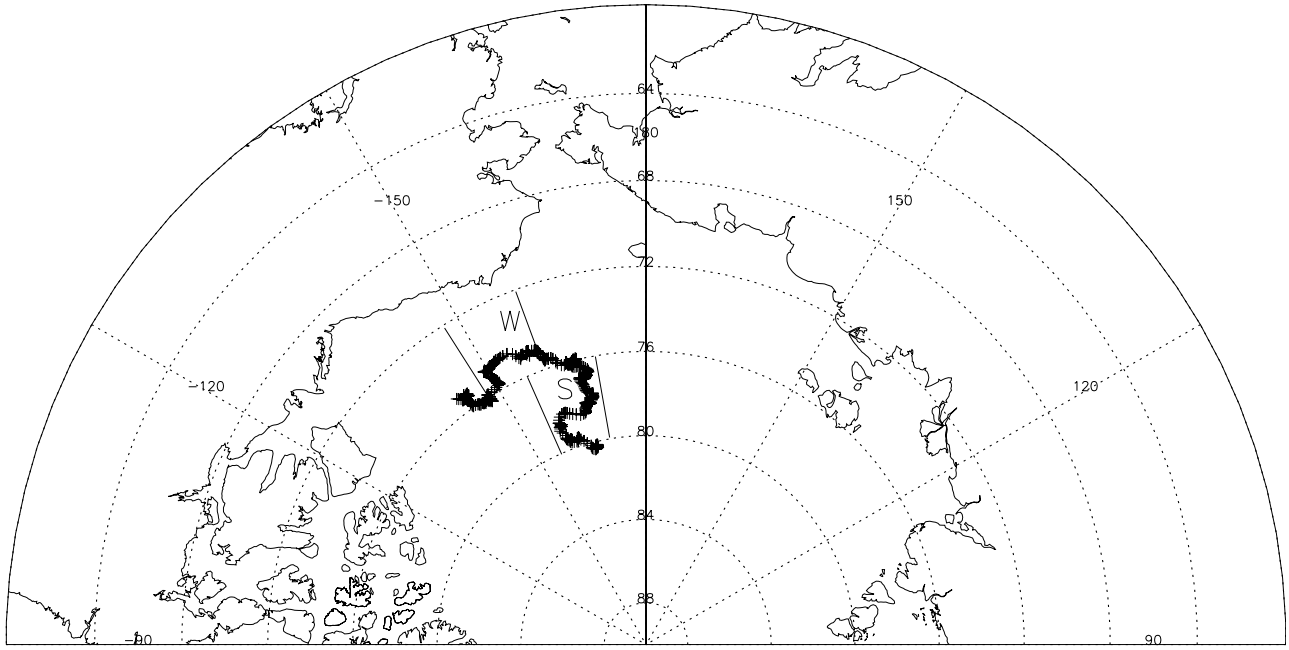

Figure 1. Map of the Arctic Ocean showing locations of the SHEBA camp and regions selected for comparisons. The area within a rectangular cell designated with "W" is the winter portion of the SHEBA track, and "S" is the summer portion.

flown on NOAA polar-orbiting satellites since late 1978 and has generated one of the longest and most complete satellite data records in existence. The 20-year global TOVS data set (1979–1998) was subsetted for the Arctic region north of 60°N, then the radiances were processed with a version of the Improved Initialization Inversion ("3I") algorithm [*Chédin et al.*, 1985; *Scott et al.*, 1999] that was modified to enhance accuracy over snow-covered and ice-covered surfaces [*Francis*, 1994]. Orbital retrievals were averaged in space to $(100\ \text{km})^2$ grid cells and in time to produce one Arctic-wide field per 24-hour period centered on 12 UTC: the so-called "Path-P" data set [*Francis and Schweiger*, 2000; *Schweiger et al.*, 2002]. The spatial grid is the same as that used for polar passive microwave products and other Arctic data sets (the Equal-Area SSM/I Earth (EASE) grid [*Armstrong and Brodzik*, 1995]).

[11] The products contained in the Path-P data set include atmospheric temperature and moisture profiles, surface skin temperature, cloud cover and height, a variety of boundary layer parameters, and sea level pressure (extracted and regridded from NCEP/NCAR Reanalyses [*Kalnay et al.*, 1996]). Path-P products have been extensively validated with measurements from various field programs and ice station data [*Schweiger et al.*, 2002]. Retrieved skin temperatures agree surprisingly well with 2-m air temperatures [*Chen et al.*, 2002] particularly given the difficulties in retrieving cloud properties in high latitudes and the interference of clouds with surface temperature retrievals. The Arctic is typically very cloudy, and when cloud cover changes, snow/ice surface temperatures often respond substantially. The RMS errors in retrieved upper-level temperatures generally decrease with height and are less than 3 K, except near the tropopause where they increase to about 4 K. Biases are less than 1.5 K at all levels and are generally slightly negative (retrievals too cold) in the upper troposphere and slightly positive in the lower troposphere.

[12] Cloud properties are much more difficult to validate. Not only are there few observations available, but conventional surface-based reports are inherently different from satellite retrievals in several ways. As viewed from the surface, low clouds may block the view of high clouds, while from space high clouds obscure low clouds. In addition, surface observers report the fraction of the sky covered by cloud with no estimate of its optical thickness, while satellite retrievals are affected by the clouds' emissivity. Despite these issues, monthly mean values of the Path-P cloud fraction have been previously compared with cloud cover estimates by surface observers and to retrievals from the International Satellite Cloud Climatology Project (ISCCP) D2 product [*Schweiger et al.*, 1999] and to lidar-retrieved cloud cover during SHEBA [*Schweiger et al.*, 2002]. While the ISCCP algorithm is apparently confounded by the extreme conditions existing in the Arctic, the Path-P product agrees well with conventional observations. The DLF values from TOVS are calculated from retrieved

Table 1. Data Sets and Variables Examined[a]

Data Sources	Variable	SHEBA Site
TOVS	Tskin	1980–1998
	CLD	1980–1998
	DLF	Oct. 1997 to Sep. 1998
GCM	Tsfc	1980–1998
	CLD	1980–1998
	DLF	1980–1998
SHEBA	Tsfc	Oct. 1997 to Sep. 1998
	CLD	Oct. 1997 to Sep. 1998
	DLF	Oct. 1997 to Sep. 1998

[a]Tsfc, near-surface air temperature; Tskin, skin temperature; CLD, cloud cover; DLF, downward longwave flux.

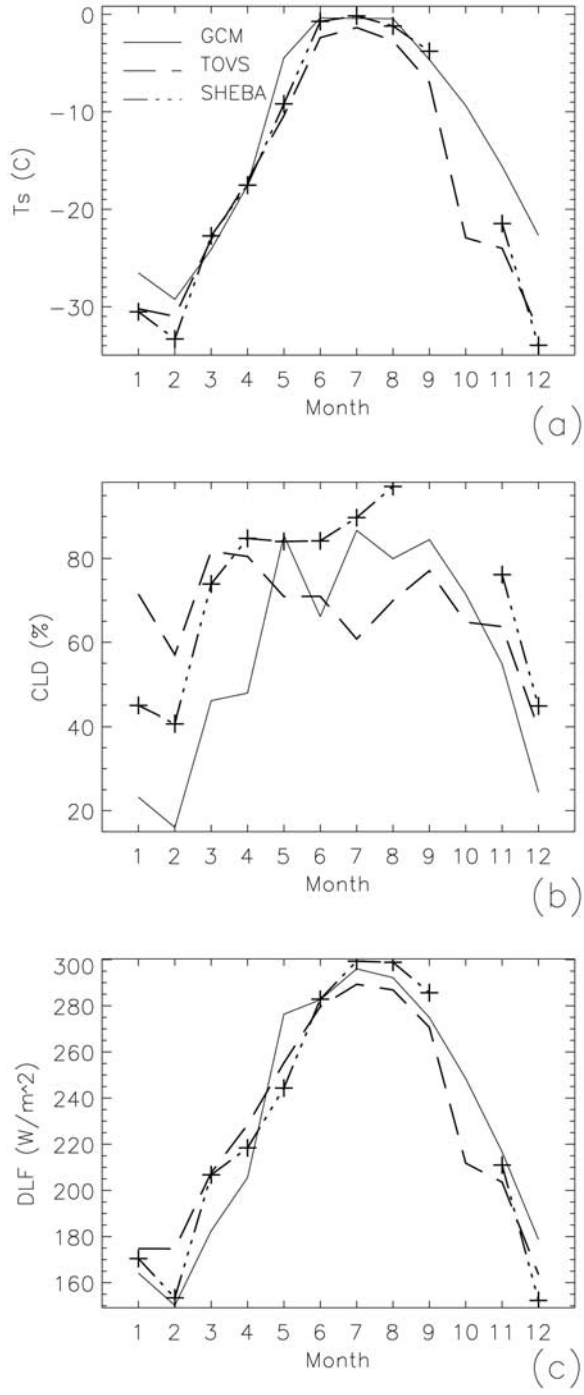

Figure 2. Annual cycles of (a) surface temperature, (b) cloud cover, and (c) downward longwave flux for SHEBA, TOVS, and GCM at the SHEBA site. All are based on 1 year (October 1997 to September 1998).

temperature and moisture profiles, cloud properties, and additional information derived from TOVS brightness temperatures [*Francis*, 1997].

[13] The SHEBA integrated data set used in this study was obtained from http://www.atmos.washington.edu/~roode/SHEBA.html. The SHEBA experiment was conducted on pack ice in the Beaufort Sea from October 1997–1998, and its goal was to provide a comprehensive observational data set for process studies, remote sensing validation, and comparison with model simulations over the Arctic Ocean [*Uttal et al.*, 2002]. Extensive field data on the atmosphere, ocean, snow and sea ice were collected during this period. The integrated SHEBA data set includes a wide range of daily atmospheric and oceanic measurements with daily temporal resolution from rawinsonde soundings, lidar, radar, meteorological surface observations, and a microwave radiometer. Variables used in this study are downward longwave flux (DLF), near-surface air temperature, and cloud cover.

4. Comparison of Climate Variables at the SHEBA Site

[14] In this section we examine and compare relationships among climate variables at the SHEBA site in the Arctic using SHEBA in situ measurements, TOVS satellite retrievals, and GCM output. The climate variables include surface air temperature (Ts; skin temperature if from TOVS), cloud cover (CLD), and DLF. These three variables are the most important ones for the surface energy budget in winter, and are more easily available from the observations. First we

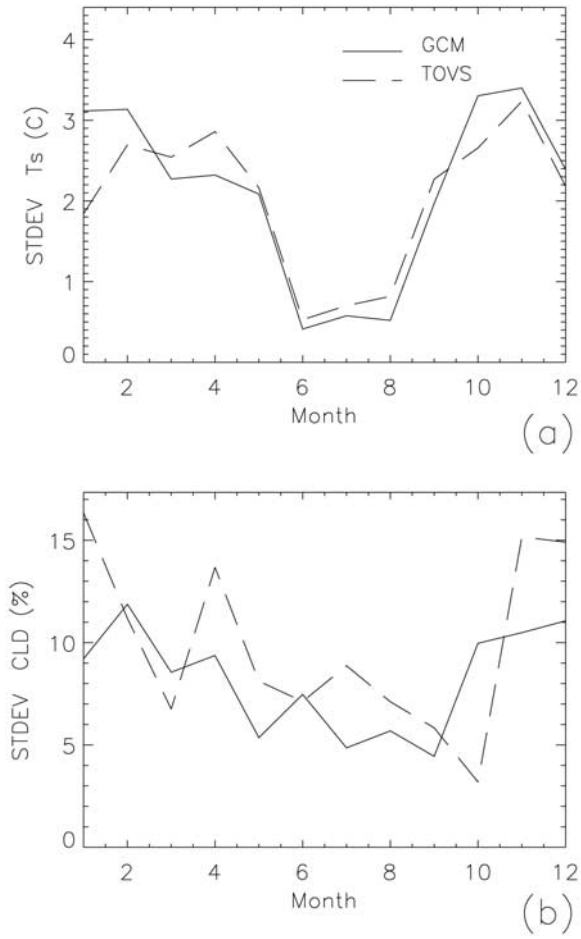

Figure 3. Interannual variability (standard deviations) of (a) surface temperature and (b) cloud cover (as in Figure 2) for TOVS and GCM based on monthly means during a 19-year record (1980–1998).

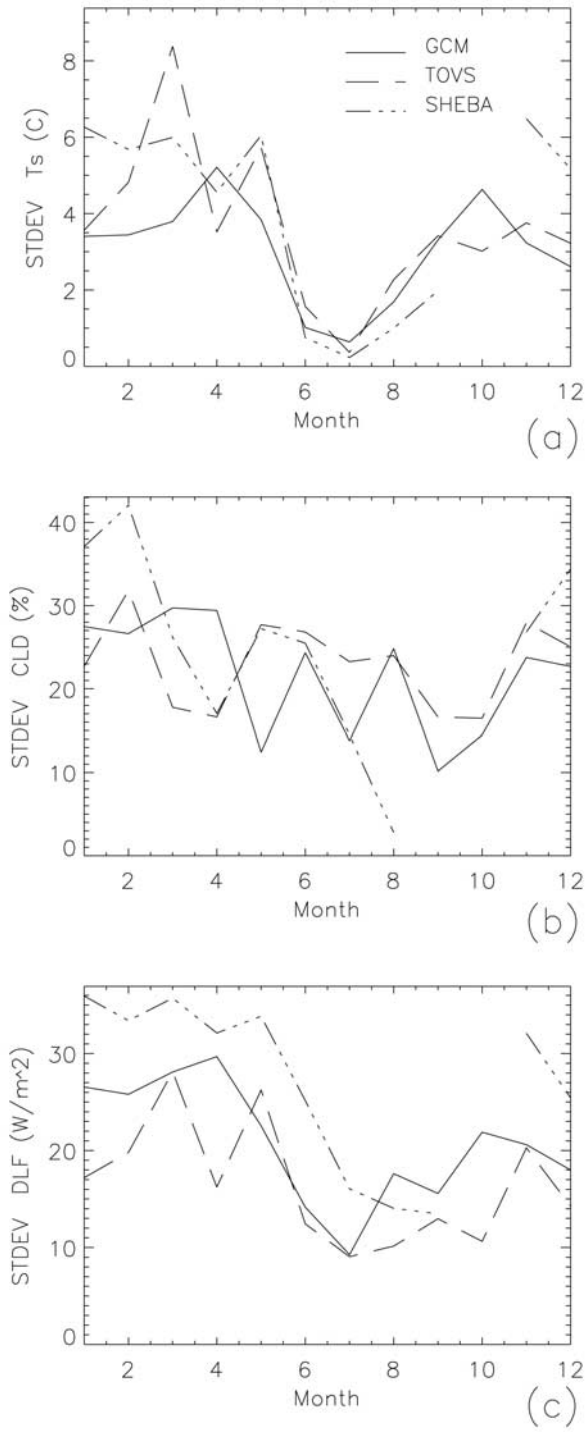

Figure 4. Daily variability (standard deviations) of (a) surface temperature, (b) cloud cover, and (c) downward longwave flux (as in Figure 2) for SHEBA, TOVS, and GCM based on daily values during the SHEBA period (October 1997 to September 1998).

compare the annual cycles, the interannual variability, and ranges of each of the variables from the three sources. We then compare relationships between pairs of variables to examine daily changes in one variable with respect to changes in another, particularly in winter months when we expect relationships among DLF, Ts, and CLD to be strongest. TOVS retrievals are available from 1979 to 1998; the corresponding 20-year period is obtained from the GCM. The region examined in this paper is shown in Figure 1 (72°–80°N, 145°–175°W). Table 1 lists the data sets and availability of parameters.

[15] Differences in the data sets should be considered while interpreting comparisons. The SHEBA surface air

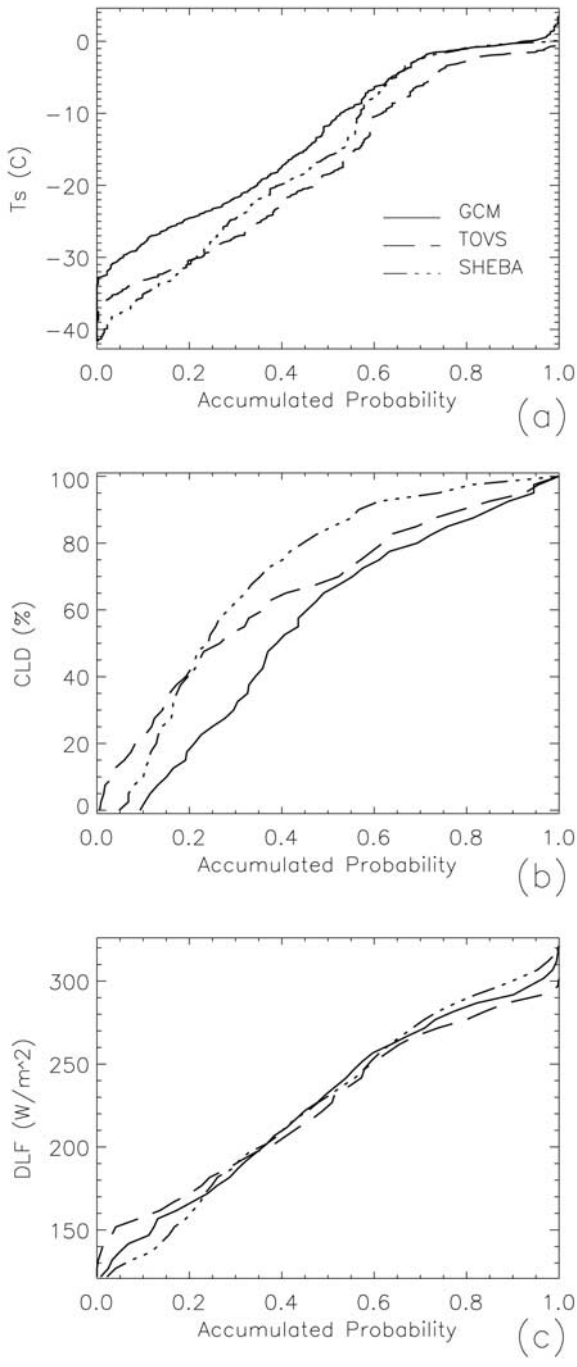

Figure 5. Accumulated probability comparisons at the SHEBA site of (a) surface temperature, (b) cloud cover, and (c) downward longwave flux. The solid line is GCM, the dashed line is TOVS, and the dash-triple-dotted line is SHEBA.

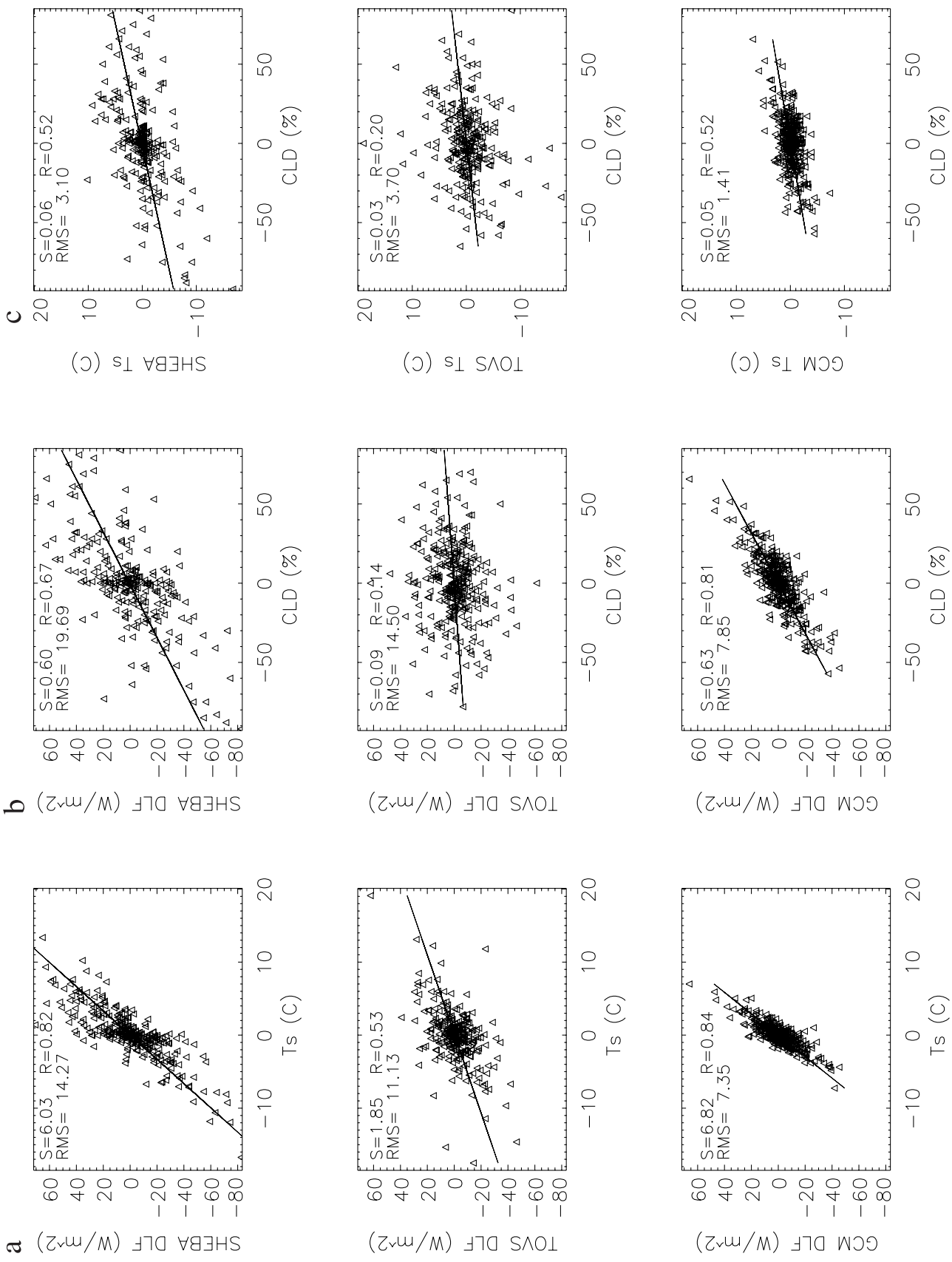
a
b
c
SHEBA DLF (W/m^2)
TOVS DLF (W/m^2)
GCM DLF (W/m^2)
Ts (C)
S=6.03 R=0.82
RMS= 14.27
S=1.85 R=0.53
RMS= 11.13
S=6.82 R=0.84
RMS= 7.35
CLD (%)
S=0.60 R=0.67
RMS= 19.69
S=0.09 R=0.14
RMS= 14.50
S=0.63 R=0.81
RMS= 7.85
SHEBA Ts (C)
TOVS Ts (C)
GCM Ts (C)
S=0.06 R=0.52
RMS= 3.10
S=0.03 R=0.20
RMS= 3.70
S=0.05 R=0.52
RMS= 1.41

temperatures are measured at 2 m above the surface, while TOVS retrieves a skin temperature. This may result in TOVS being 1°–2° colder than SHEBA primarily in fall, winter, and spring when near-surface temperature inversions are common. Hereafter, we use the term "surface temperature" and the symbol Ts for all three data sets with the understanding that SHEBA and GCM values are near-surface air temperatures and TOVS is the skin temperature. The SHEBA values are measured at a point and averaged over 24 hours, while the TOVS and GCM values are area averaged over the SHEBA track with a spatial resolution of $(100\ \text{km})^2$ and $5° \times 4°$, respectively. The mismatch of scales is unavoidable in validating coarse model output with surface-based point measurements. However, we expect that relationships between climate variables should be less affected by differing spatial scales than are comparisons of absolute values. For the annual analysis, GCM variables are averaged over the whole SHEBA region (seven grid cells). For winter and summer the GCM values are averaged over three grid cells (see Figure 1). Observations from the SHEBA experiment are for 1 year only (October 1997 to September 1998). The TOVS and GCM values correspond to SHEBA dates. Although it is important to note that the 1-year GCM record for this period is not meant to correspond to the actual conditions during that 1 year, the model's monthly means of DLF, Ts, and CLD for this period are representative of the average climatology of the decade surrounding it.

4.1. Annual Cycles and Interannual Variability

[16] Figure 2 shows the annual cycles of the three climate variables at the SHEBA site for each data set. Figure 2a shows that for all three data sets the annual range of surface temperature is large with a maximum near 0°C in summer when the surface is melting. In winter the GCM's surface temperature is warmer than TOVS and SHEBA temperatures. The largest discrepancy among data sets occurs for cloud cover (Figure 2b). As mentioned in section 3, the definition of cloud is different for each data set. The GCM values do not include clouds with modeled optical depths less than 1, and TOVS cloud retrievals may include low-level ice clouds or so called "diamond dust", while the surface observers do not. This may explain the GCM underestimating and the TOVS exceeding SHEBA values in winter when diamond dust and thin clouds are common [*Curry et al.*, 1996]. The amplitude of the GCM's annual cycle is much larger than that of either TOVS or SHEBA. For the GCM, cloud cover ranges between 15–85%, for SHEBA between 40–100%, and for TOVS between 40–80%. The GCM's annual cycle is more similar to the SHEBA observations with a minimum in winter and maximum in summer than it is to TOVS, which is fairly uniform throughout the year. The GCM is more consistent with surface-based observations [*Huschke*, 1969] with large seasonal changes and low cloud cover in winter [*Miller and Russell*, 2002]. However, when the Huschke climatology is modified to include diamond dust [*Curry et al.*, 1996], there is better agreement with the TOVS annual cycle.

[17] An important climate variable for the Arctic energy budget is the downward longwave flux (DLF). Figure 2c shows that the amplitudes of the annual cycles in all three data sets are in good agreement, with maxima near 300 W/m^2 in summer and minima near 160 W/m^2 in winter. This suggests that the longwave component of the GCM's energy budget is well simulated despite the large differences in cloud cover. With additional variables and further sensitivity analyses, we expect to resolve this issue. The DLF obtained from TOVS is also in good agreement with in situ SHEBA measurements. The amplitude of the annual cycle for TOVS is somewhat lower than for SHEBA, as it is about 10 W/m^2 too low in summer and too high in winter. This is expected given the much coarser spatial resolution of TOVS retrievals and consequent reduction in variability. The similarity of the DLF cycle to the surface temperature cycle is consistent with other observations; these variables are closely related, especially in winter [*Guest and Davidson*, 1994].

[18] In addition to comparing monthly means of the climate variables as in Figure 2, it is important to understand the variability and covariability of the parameters. We examine both the daily variability within a given month and the interannual variability. On the basis of monthly means from 1980 to 1998, Figures 3a and 3b show that the GCM's interannual variability in both surface temperature and cloud cover agrees well with TOVS, with the greatest variability occurring in winter. Surface temperatures are close to the melting point during summer in the Arctic, and the variability is small.

[19] Figure 4 displays the standard deviations of the daily values in each month for the three data sets. The daily variability of the TOVS and GCM surface temperature is smaller than that of SHEBA in winter and spring (Figure 4a). For most of the year, TOVS and the GCM have a smaller daily variability in downward longwave flux than does SHEBA. All three data sets show the largest variability in winter and smallest in summer for surface temperature and DLF. Again, the largest discrepancy in patterns among the three data sets is in the cloud cover.

4.2. Accumulated Probability

[20] The ranges of variable magnitudes are compared among the three data sets by examining the accumulated probabilities presented in Figure 5. The abscissa in Figure 5 shows the probability that a variable is less than a given value on the ordinate. Because the 1-year model daily record is not meant to correspond to actual measurements during that year, Figure 5 illustrates the GCM's ability to represent the range of the actual climate.

Figure 6. (opposite) Covariability in daily changes of pairs of climate variables for each data source: (top) SHEBA, (middle) TOVS, and (bottom) GCM. (a) Comparisons of daily changes in surface temperature and downward longwave flux. (b) Fractional cloud cover and downward longwave flux. (c) Surface temperature and cloud cover. Each point represents the day-to-day change in one variable versus the corresponding change in the second variable for the same day at the SHEBA site (October 1997 to September 1998). The legend in each plot consists of two lines: The first line is S = regression slope and R = correlation coefficient; the second line is RMS = the RMS difference.

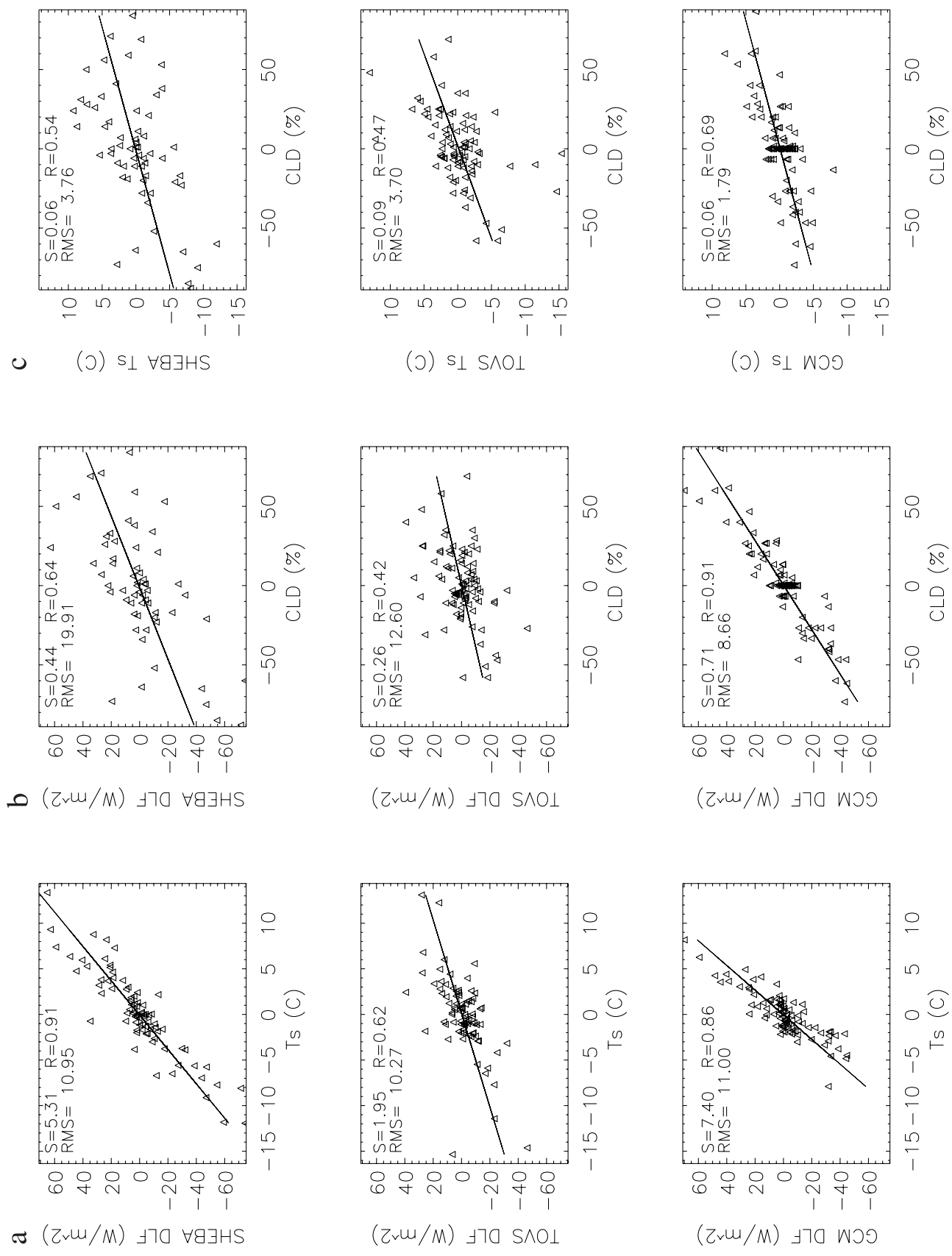

Figure 7. Same as Figure 6, except for winter (December–February).

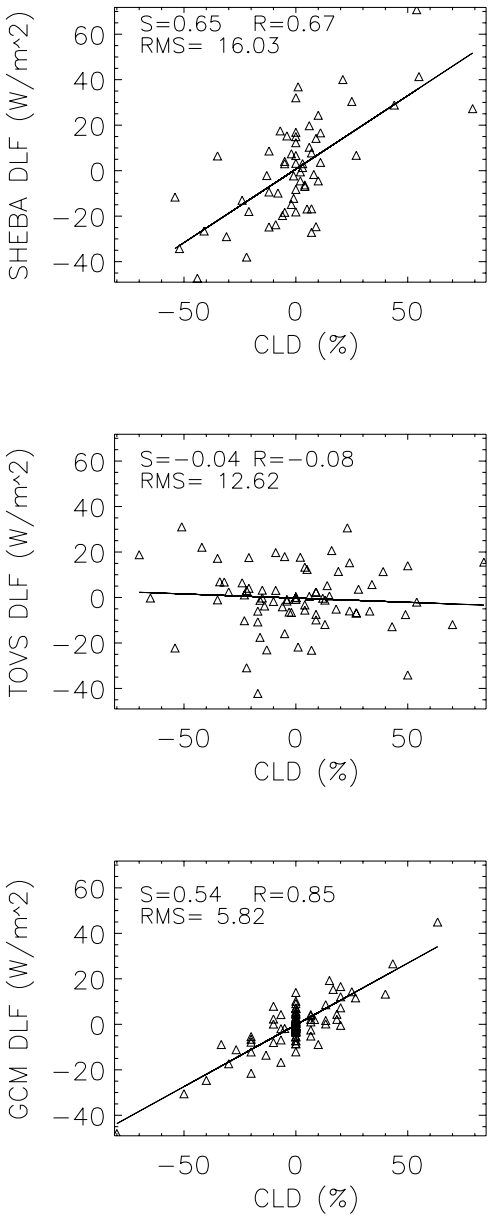

Figure 8. Same as Figure 6, except for summer (June–August) and only for the relationship between downward longwave flux and cloud cover.

[21] For each of the three variables, the ranges of TOVS values are smaller than those for SHEBA measurements. As expected, DLF and Ts are high (low) when cloud amount is high (low). The agreement among the three data sets is surprisingly good for DLF. The GCM's surface temperature, however, is too high in colder conditions. The GCM has many more clear days and always has fewer clouds than observed. For low values of cloud cover, Figure 5 shows that the modeled DLF and surface temperature are higher than the SHEBA-observed values even though the modeled cloud cover is lower than observed. This apparent inconsistency occurs, in part, because the GCM cloud cover includes only clouds with optical depths exceeding 1, while all optical depths are included in the calculations of DLF. This leads to the GCM's DLF being larger than would be expected in modeled clear conditions, which leads to higher than expected surface temperatures. In general, however, DLF and surface temperature are consistent among the three data sets.

4.3. Relationships Between Daily Changes

[22] To approach the question of how relationships and sensitivities among variables contribute to climate processes and feedbacks in the Arctic, we examine covariability between pairs of climate variables. The regression slope or sensitivity of these relationships can be used in the classical feedback analysis formulation to estimate climate feedbacks [*Hansen et al.*, 1984]. If the different types of observations (in situ and satellite) and the GCM show similar relationships among climate variables, then we have greater confidence that both TOVS satellite retrievals and the GCM can be used to investigate Arctic climate feedbacks. Where there are discrepancies in the nature of the relationships, we attempt to discover why.

[23] To investigate these relationships, we use daily mean values from the three data sets. Figure 6 shows the comparison of the daily changes for SHEBA, TOVS and the GCM during the 1-year SHEBA experiment. Each point represents the day-to-day change in one variable versus the corresponding change in the second variable. For example, Figure 6a indicates that the daily change in DLF is highly linearly correlated (greater than 0.8 for SHEBA and the GCM) with the daily change in surface temperature for the three data sets. Furthermore, these same panels quantify the relationship and show that for SHEBA measurements, the DLF changes by 6.0 W/m^2 for every degree change in surface temperature and 6.8 W/m^2 for the GCM. For TOVS, the change in DLF is much smaller (1.9 W/°C m^2). This is likely caused by the fact that the TOVS retrieval algorithm rejects the cloudiest cases, thus some of the largest changes are omitted from the TOVS data set. All the slopes are significant at the 95% confidence level. The agreement between the GCM and SHEBA observations is encouraging for evaluation of climate feedbacks.

[24] The results in Figure 6a cannot, by themselves, yield the cause and effect relationship between temperature and DLF. Does the surface temperature increase because the DLF increases, or does the DLF increase because the surface temperature increases? The positive feedback between the two variables is well known. If there is a positive perturbation in one of the two variables, it will cause the other variable to increase, but something else keeps them in check. We examined lag-lead relationships between pairs of daily-averaged variables, but we found no significant correlations at this time interval. These correlations might become significant if the variables are averaged over shorter periods than 1 day. Ultimately, multivariate relationships must be examined to explain system feedbacks, but understanding the relationships between pairs of climate variables is a necessary first step.

[25] Figure 6b shows that daily changes in DLF and cloud cover are highly correlated for both SHEBA observations and the GCM, with DLF increasing by 0.6 W/m^2 for each percent increase in cloud cover. Another feature of the GCM's relationship is that there is much less scatter about the regression line, which indicates that the values are less sensitive to other variables not taken into account in this

study. This suggests that the GCM's relationships are more simple and deterministic than the real world. The range of the GCM's daily changes is smaller than that of SHEBA for each of the variables. For SHEBA the daily changes in DLF exceed 60 W/m^2 while for the GCM they only reach 40 W/m^2. Similarly for cloud cover there are many days when the in situ SHEBA observations change by more than 50%, while the GCM's daily changes are smaller. This is likely due to the comparison of point measurements at SHEBA with a spatially averaged value from the GCM (seven grid cells). For TOVS, the correlation between DLF and cloud cover is very low. Given the good agreement of TOVS surface temperature and DLF with SHEBA measurements, the low correlation may result from variability in cloud emissivity being inextricably included in TOVS cloud cover retrievals.

[26] We expect that there could be large differences in the relationships shown in Figure 6 if winter and summer are examined separately. Because there is no solar radiation during winter, one would expect the correlation between surface temperature and DLF to be higher. Figure 7 is consistent with expectations in showing higher winter correlations for all of the relationships presented in Figure 6. One of the interesting features is that the change in DLF per unit change in surface temperature is now larger for the GCM than for the observations (7.4 W/m^2/°C versus 5.3 W/°C m^2). Compared to annual values, the GCM slope has increased and SHEBA has decreased. The change in TOVS is much smaller than for either the SHEBA observations or the GCM, but the correlation coefficient has increased much more for TOVS than for the others. This is likely due to reduced rejections of TOVS retrievals for heavy overcast conditions, as thick clouds are less prevalent in winter.

[27] In summer, changes in DLF are still related to changes in cloud cover as indicated in Figure 8 from SHEBA and GCM data. Large increases in DLF are correlated with increases in cloud cover. The inability of TOVS to retrieve surface temperature and DLF in overcast conditions is the likely reason for TOVS relationships differing from the other two, as thick stratus clouds are common in summer. Relationships between cloud cover and the other climate variables differ among the three data sets. One possible reason is that cloud cover might not be the best cloud variable to use. Perhaps cloud base height or cloud optical depth would be more elucidating, but these variables are not readily available. Because surface temperature changes in summer are always near zero, we would expect little correlation between surface temperature and other variables. With such small daily increments in surface temperature, the linear regression is not robust and the resulting slope is not reliable, and therefore is not shown.

[28] The relationships in this section are based on 1 year of observations and 1 year of GCM output. Because we have 22 years of GCM output, we can examine the interannual variability of the model's relationships between variables. Figure 9 presents a time series of the GCM's wintertime relationship between DLF and surface temperature from 1979 to 2000. Figure 9 is constructed by selecting GCM grid cells that contain the SHEBA winter site and regressing DLF against surface temperature for each of the 22 winters (mean of December, January, and February). Figure 9 shows significant variation in the relationship from year to year, with a minimum value of the regression slope of 4.9 W/m^2/°C and a maximum of 7.4 W/m^2/°C, which happens to be the winter of the SHEBA year, even though the anomalies of individual variables are near zero. The average regression slope during the 22-year period is 6.1 W/m^2/°C, which is closer to the regression slope calculated from SHEBA measurements (5.3 W/m^2/°C). We cannot calculate the interannual variability of this relationship from the observations because we only have 1 year of data from SHEBA, but future work will include a calculation from Russian "North Pole" station data, which could be illuminating.

5. Discussion and Conclusions

[29] A standard method of evaluating a GCM's representation of the real climate is to compare simulated climate variables with observations of the same variables. Figures 2–5 illustrate such comparisons for monthly means and standard deviations of surface temperature, cloud cover, and downward longwave flux. The GCM output is generally consistent with both in situ SHEBA measurements and TOVS satellite retrievals except for cloud cover, which is attributable, in part, to the differences in the way clouds are defined in the three sources.

[30] The seasonal cycles of surface temperature and downward longwave flux are also consistent among the three data sets. Again, there are significant differences in cloud cover. Inclusion of diamond dust in TOVS cloud cover retrievals may account for its values exceeding those from both GCM and SHEBA values in winter. Underestimates by the GCM likely result from its cloud fractions including only clouds with optical depths larger than 1.

[31] This standard validation method is informative, but only tells part of the story related to investigations of feedback processes. Feedbacks involve relationships and sensitivities among variables, hence our focus on the covariability of three climatically important quantities in this study. For a model to represent feedbacks correctly, it must represent relationships and sensitivities among variables correctly. Moreover, the GCM's ability to provide plausible scenarios of future climate change also depends on the realism of these relationships. To address this point, we compare the covariability among three variables (surface temperature, cloud cover, and DLF) to evaluate the GCM's performance. The results are encouraging.

[32] Table 2 summarizes the relationships between pairs of climate variables at the SHEBA site. Slopes of the regression lines for each pair are given, with the correlations in parentheses. An asterisk after a correlation indicates that it is not significant at the 95% confidence level. The highest correlations occur for the relationships between DLF and surface temperature in winter for both the GCM and the in situ SHEBA data and between DLF and cloud cover for the GCM. The linear correlations for TOVS are somewhat lower, likely because of the lack of retrievals in overcast conditions. In winter the change in DLF per unit change in temperature is lowest for TOVS (2.0 W/m^2/°C) and highest for the GCM (7.4 W/m^2/°C) as compared to the SHEBA value of 5.3 W/m^2/°C. In summer the correlations between DLF and cloud cover are high for the GCM and SHEBA, but the correlation for TOVS is low and shows no relation-

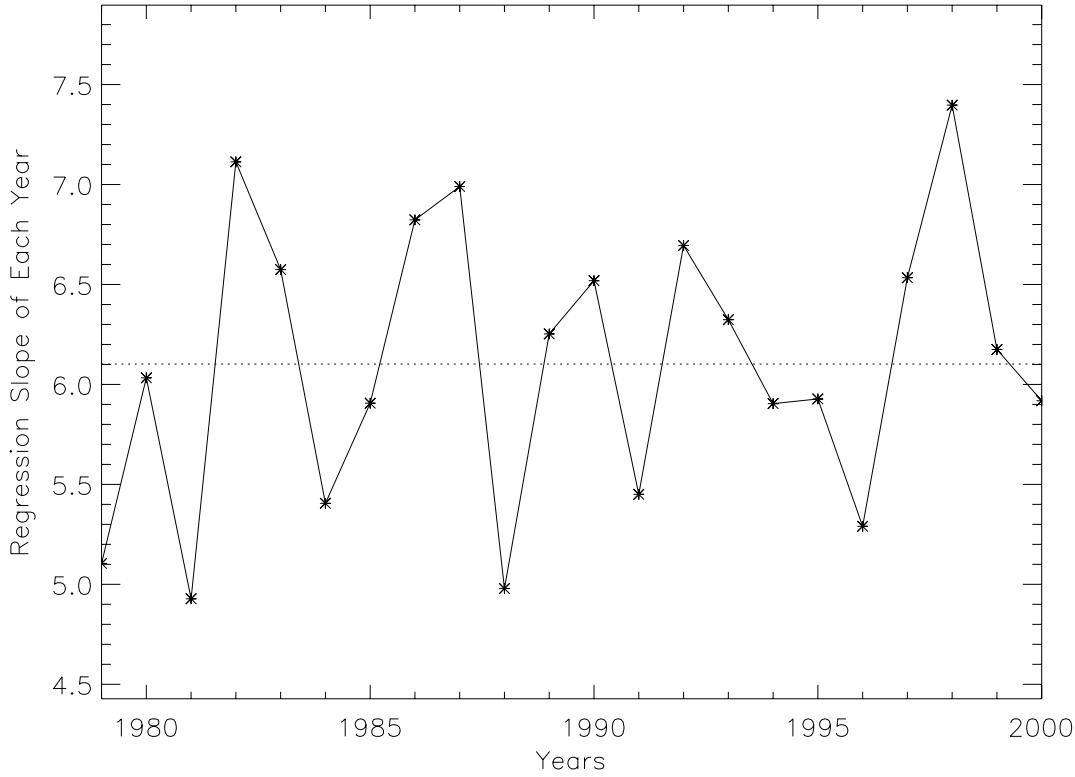

Figure 9. Time series of the GCM regression slope for daily changes in DLF against those in surface temperature during winter (DJF) for 1979–2000 over the SHEBA site.

ship between the two variables. This supports our possible explanation for lower correlation between TOVS variables because in summer, cloud cover is largest, TOVS rejection rates are highest, and thus TOVS covariabilities omit some of the largest daily changes.

[33] *Chiacchio et al.* [2002] performed a sensitivity study on the likely errors in DLF resulting from uncertainty in various parameters using a radiative transfer model called Streamer [*Key and Schweiger*, 1998]. The sensitivity of DLF to perturbations in the surface temperature for standard Arctic winter and summer conditions is 1.3 W/m^2/°C and 2.8 W/m^2/°C. These numbers are much smaller than those we obtain from both SHEBA and the GCM. There are several possible reasons why the Chiacchio values are smaller than observed sensitivities. The most likely is that they examine the corresponding changes in DLF given changes in one particular variable by holding constant all other variables. In the real world, every climate parameter may change simultaneously. Our results are more realistic in this sense. *Chiacchio et al.* [2002] also point out that surface temperature, cloud cover, and cloud base height are indeed among the factors to which DLF is most sensitive.

[34] Table 2 shows that all three data sets indicate a high correlation between temperature and cloud cover in winter. Not only are the correlations high, the magnitudes of the responses are also similar, ranging between 0.06° and

Table 2. Relationships Between Variable Pairs by Season and Data Set

	SHEBA		TOVS		GCM	
Season	Slope of Regression Line	Correlation Coefficient	Slope of Regression Line	Correlation Coefficient	Slope of Regression Line	Correlation Coefficient
			DLF versus Ts, W/m^2/°C			
Annual	6.0	0.82	1.9	0.53	6.8	0.84
Winter	5.3	0.91	2.0	0.62	7.4	0.86
Summer	17.7	0.65	−0.6	−0.12[a]	−0.0	0.0[a]
			DLF versus CLD, W/m^2/%			
Annual	0.6	0.67	0.1	0.14	0.6	0.81
Winter	0.4	0.64	0.3	0.42	0.7	0.91
Summer	0.7	0.67	−0.04	−0.08[a]	0.5	0.85
			Ts versus CLD, °C/%			
Annual	0.06	0.52	0.03	0.20	0.05	0.52
Winter	0.06	0.54	0.09	0.47	0.06	0.69
Summer	0.00	0.17[a]	−0.03	−0.39	−0.01	−0.31

[a]Nonsignificance at the 95% confidence level.

0.09°C per percent change in cloud cover. As expected, the relationship is much weaker in summer and not reliable. There are several reasons for the differences between these relationships in summer and winter. First, there is no solar radiation in winter, thus DLF is primarily controlled by cloud emission. More cloud cover reemits more longwave radiation back to the surface. Second, the surface temperature over the Arctic Ocean changes little in summer because it is confined to near the melting point of snow and sea ice. This constraint of the surface temperature in summer explains why the high correlation between DLF and cloud cover is not accompanied by a similar response between cloud cover and surface temperature. In summer the increased DLF in heaviest overcast will be partially compensated by decreased downward shortwave radiation.

[35] In our study, this method of evaluating the GCM's output by comparing the relationships and sensitivities among pairs of climate variables provides additional useful and valuable information beyond the standard comparison methods. By looking at these covariabilities, we can begin to identify physically based causes for agreement and disagreement and to focus on physical processes that should be more carefully investigated. Both TOVS satellite retrievals and GCM output are compared with the in situ SHEBA measurements in this investigation. Standard comparisons with observations (Figures 2–5) show that TOVS satellite retrievals agree with SHEBA quite well. However, investigations of the relationships between pairs of variables weaken this consistency, and its shortcomings are highlighted in daily relationship comparisons. TOVS always has much weaker relationships between each pair of variables compared to SHEBA and the GCM, especially those involving the cloud cover, which we believe is largely caused by the lack of retrievals under overcast conditions: the cases with large $\Delta DLF/\Delta Ts$ will be missed because they occur when thick clouds come and go. The TOVS cloud cover retrievals in polar conditions are being updated and improved. We hope to apply the same study to the new version of TOVS when it is available to see whether the relationships remain the same.

[36] Our results indicate that the GCM provides a reasonable representation of both the annual cycles and the variability of three selected climate variables. There is also good agreement with observations when we compare relationships between daily changes of climate variables. This brings us a step closer to understanding the feedbacks that operate in the Arctic and are believed to make the region sensitive to climate change. Our results provide additional confidence in future climate change scenarios obtained from the model. The relationships are stronger than observed, however, which indicates the potential influences of unrealistic, missing and/or incomplete parameterizations in the GCM.

[37] This paper describes another method to evaluate a model's ability to simulate climate processes. The Arctic is a data sparse area for which long-term, basin-wide, comprehensive, and accurate data sets are not available at present. The results from this study provide confidence in the GISS GCM's ability to simulate the relationships between climate variables, and to simulate climate change in response to increasing atmospheric greenhouse gases [e.g., *Miller and Russell*, 2000, 2002]. While many issues still remain, it is clear that progress has been made, and an alternative method of evaluating a model's representation has been demonstrated.

[38] Finally, we note that the relationships and sensitivities between climate variables are not fixed over time and space. By comparing the temporal evolution and spatial pattern of the relationships in model output with the corresponding covariability in observed values, we obtain a better understanding of model sensitivities and open a new window for evaluating the performance of a global climate model. *Aires and Rossow* [2003] provide an encouraging theoretical framework for this next step.

[39] **Acknowledgments.** This work is supported by NASA grant NAG5-11720 and by a graduate research assistantship from the Institute of Marine and Coastal Sciences at Rutgers University. Partial support for JRM has been provided by Project #32103 of the New Jersey Agricultural Experiment Station. We are grateful to Dr. William B. Rossow for constructive discussion and to Stephen J. Vavrus and another reviewer for helpful comments. We would like to thank Dr. Stephan de Roode for consultation regarding the SHEBA data. We also thank Elias Hunter for computing support.

References

Aires, F., and W. B. Rossow, Inferring instantaneous, multivariate and nonlinear sensitivities for the analysis of feedback processes in a dynamical system: The Lorenz model case study, *Q. J. R. Meteorol. Soc.*, *129*, 239–275, 2003.

Armstrong, R. L., and M. J. Brodzik, An Earth-gridded SSM/I data set for cryospheric studies and global change monitoring, *Adv. Space Res.*, *16*(10), 155–163, 1995.

Chédin, A., N. A. Scott, C. Wahiche, and P. Mouliner, The improved initialization inversion method: A high resolution physical method for temperature retrievals from satellites of the TIROS-N series, *J. Clim. Appl. Meteorol.*, *24*, 128–143, 1985.

Chen, Y., J. A. Francis, and J. R. Miller, Surface temperature of the Arctic: Comparison of TOVS satellite retrievals with surface observations, *J. Clim.*, *15*, 3698–3708, 2002.

Chiacchio, M., J. A. Francis, and P. Stackhouse Jr., Evaluation of methods to estimate the surface downwelling longwave flux during Arctic winter, *J. Appl. Meteorol.*, *41*, 307–318, 2002.

Curry, J. A., W. B. Rossow, D. Randall, and J. L. Schramm, Overview of Arctic cloud and radiation characteristics, *J. Clim.*, *9*, 1731–1764, 1996.

Francis, J. A., Improvements to TOVS retrievals over sea ice and applications to estimating Arctic energy fluxes, *J. Geophys. Res.*, *99*, 10,395–10,408, 1994.

Francis, J. A., A method to derive downwelling longwave fluxes at the Arctic surface from TIROS operational vertical sounder data, *J. Geophys. Res.*, *102*, 1795–1806, 1997.

Francis, J. A., and A. J. Schweiger, A new window opens on the Arctic, *Eos Trans AGU*, *81*(8), 77–78, 2000.

Gates, W. L., et al., An overview of the results of the Atmospheric Model Intercomparison Project (AMIP I), *Bull. Am. Meteorol. Soc.*, *80*, 29–55, 1999.

Guest, P., and K. L. Davidson, Factors affecting variations of snow surface temperature and air temperature over sea ice in winter, in *The Polar Oceans and Their Role in Shaping the Global Environment*, *Geophys. Monogr. Ser.*, vol. 85, edited by O. M. Johannessen, R. D. Muench, and J. E. Overland, pp. 435–442, AGU, Washington, D. C., 1994.

Hansen, J., G. Russell, D. Rind, P. Stone, A. Lacis, S. Lebedeff, R. Ruedy, and L. Travis, Efficient three-dimensional global models for climate studies: Models I and II, *Mon. Weather Rev.*, *111*, 609–662, 1983.

Hansen, J., A. Lacis, D. Rind, G. Russell, P. Stone, I. Fung, R. Ruedy, and J. Lerner, Climate sensitivity: Analysis of feedback mechanisms, in *Climate Processes and Climate Sensitivity*, *Geophys. Monogr. Ser.*, vol. 29, edited by J. E. Hansen and T. Takahashi, pp. 130–163, AGU, Washington, D. C., 1984.

Holland, M. M., and C. M. Bitz, Polar amplification of climate change in coupled models, *Clim. Dyn.*, *21*, 221–232, doi:10.1007/s00382-003-0332-6, 2003.

Huschke, R., Arctic cloud statistics from "air-calibrated" surface weather observations, *Rep. RM-6173-PR*, 79 pp., Rand Corp., Santa Monica, Calif., 1969.

Ingram, W. J., C. A. Wilson, and J. F. B. Mitchell, Modelling climate change: An assessment of sea ice and surface albedo feedbacks, *J. Geophys. Res.*, *94*, 8609–8622, 1989.

Intergovernmental Panel on Climate Change, Model evaluation, in *Climate Change 2001: The Scientific Basis-Contribution of Working Group I to the Third Assessment Report of the Intergovernmental Panel on Climate Change*, edited by J. T. Houghton et al., pp. 471–524, Cambridge Univ. Press, New York, 2001.

Kalnay, E., et al., The NCEP/NCAR 40-year reanalysis project, *Bull. Am. Meteorol. Soc.*, *77*, 437–471, 1996.

Key, J., and A. J. Schweiger, Tools for atmospheric radiative transfer: Streamer and FluxNet, *Comput. Geosci.*, *24*, 443–451, 1998.

Large, W. G., J. C. McWilliams, and S. C. Doney, Oceanic vertical mixing: A review and a model with a nonlocal boundary layer parameterization, *Rev. Geophys.*, *32*, 363–403, 1994.

Maslanik, J., C. Fowler, T. Scambos, J. Key, and W. Emery, AVHRR-based polar pathfinder products for modeling applications, *Ann. Glaciol.*, *25*, 388–392, 1997.

McGinnis, D. L., and R. Crane, A multivariate analysis of Arctic climate in GCMs, *J. Clim.*, *7*, 1240–1250, 1994.

Miller, J. R., and G. L. Russell, Investigating the interactions among river flow, salinity and sea ice using a global coupled atmosphere-ocean-ice model, *Ann. Glaciol.*, *25*, 121–126, 1997.

Miller, J. R., and G. L. Russell, Projected impact of climate change on the freshwater and salt budgets of the Arctic Ocean by a global climate model, *Geophys. Res. Lett.*, *27*, 1183–1186, 2000.

Miller, J. R., and G. L. Russell, Projected impact of climate change on the energy budget of the Arctic Ocean by a global climate model, *J. Clim.*, *15*, 914–928, 2002.

Rind, D., R. Healy, C. P. Parkinson, and D. Martinson, The role of sea ice in $2 \times CO_2$ climate model sensitivity. Part I: The total influence of sea ice thickness and extent, *J. Clim.*, *8*, 449–463, 1995.

Russell, G. L., J. R. Miller, and D. Rind, A coupled atmosphere-ocean model for transient climate change studies, *Atmos. Ocean*, *33*, 683–730, 1995.

Schweiger, A. J., R. W. Lindsay, J. R. Key, and J. A. Francis, Arctic clouds in multiyear satellite data sets, *Geophys. Res. Lett.*, *26*, 1845–1848, 1999.

Schweiger, A. J., R. W. Lindsay, J. A. Francis, J. Key, J. M. Intrieri, and M. D. Shupe, Validation of TOVS Path-P data during SHEBA, *J. Geophys. Res.*, *107*(C10), 8041, doi:10.1029/2000JC000453, 2002.

Scott, N. A., A. Chédin, R. Armante, J. A. Francis, C. Stubenrauch, J. P. Chaboureau, F. Chevallier, C. Claud, and F. Cheruy, Characteristics of the TOVS Pathfinder Path-B dataset, *Bull. Am. Meteorol. Soc.*, *80*, 2679–2701, 1999.

Serreze, M. C., Observational evidence of recent change in the northern high-latitude environment, *Clim. Change*, *46*, 159–207, 2000.

Uttal, T., et al., The surface heat budget of the Arctic Ocean, *Bull. Am. Meteorol. Soc.*, *83*, 255–276, 2002.

F. Aires and G. L. Russell, NASA/Goddard Institute for Space Studies, 2880 Broadway, New York, NY 10025, USA. (filipe@sharki.giss.nasa.gov; grussell@giss.nasa.gov)

Y. Chen, J. A. Francis, and J. R. Miller, Institute of Marine and Coastal Sciences, Rutgers University, 71 Dudley Road, New Brunswick, NJ 08901, USA. (chen@imcs.rutgers.edu; francis@imcs.rutgers.edu; miller@arctic.rutgers.edu)